AIP Applied Physics Letters

Barrier-width dependence of quantum efficiencies of GaN/Al x Ga 1x N multiple quantum wells

Eun-joo Shin, J. Li, J. Y. Lin, and H. X. Jiang

Citation: Applied Physics Letters **77**, 1170 (2000); doi: 10.1063/1.1289262
View online: http://dx.doi.org/10.1063/1.1289262
View Table of Contents: http://scitation.aip.org/content/aip/journal/apl/77/8?ver=pdfcov
Published by the AIP Publishing

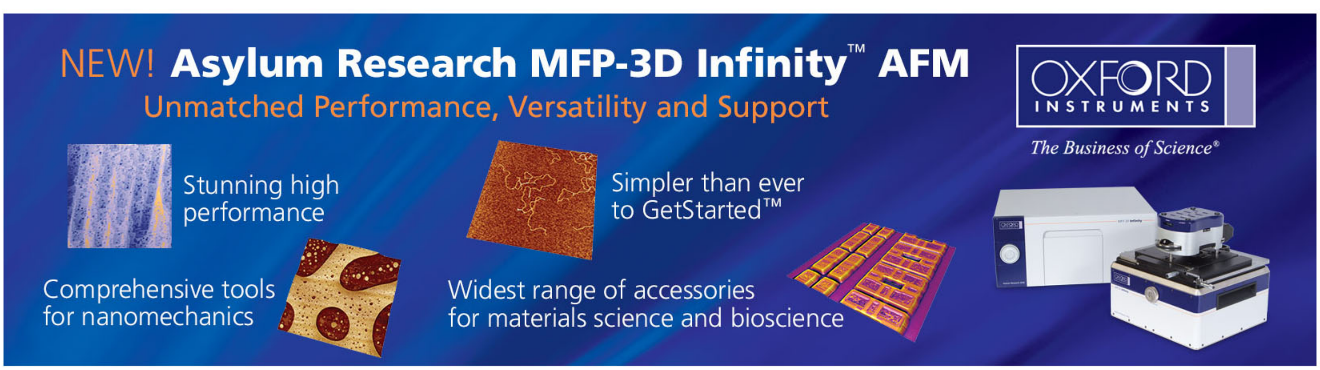

Barrier-width dependence of quantum efficiencies of GaN/$Al_xGa_{1-x}N$ multiple quantum wells

Eun-joo Shin,[a] J. Li, J. Y. Lin, and H. X. Jiang[b]
Department of Physics, Kansas State University, Manhattan, Kansas 66506-2601

(Received 10 April 2000; accepted for publication 22 June 2000)

We present the results of picosecond time-resolved photoluminescence (PL) measurements for a set of 30 Å well GaN/$Al_xGa_{1-x}N$ $(x\sim 0.2)$ multiple-quantum-well (MQW) structures with varying barrier widths L_B from 30 to 100 Å, grown by metalorganic chemical-vapor deposition. The PL quantum efficiency and the recombination lifetime of these MQWs were observed to increase monotonously with an increase of the barrier width up to 80 Å. These behaviors were explained by considering two distinct mechanisms that control the radiative recombination efficiencies in MQWs. When the barrier width is below the critical thickness, the nonradiative recombination rate increases with a decrease of the barrier width due to enhanced probabilities of the electron and hole wave functions at the interfaces as well as in the AlGaN barriers. On the other hand, the misfit dislocation density increases as the barrier width approaches the critical thickness, which can result in an enhanced nonradiative interface recombination rate. Our studies here have shown that the optimal GaN/AlGaN $(x\sim 0.2)$ MQW structures for UV light-emitter applications are those with barrier widths ranging from 40 to 80 Å. © *2000 American Institute of Physics.* [S0003-6951(00)00534-9]

The group-III-nitride semiconductors consisting of AlN, GaN, InN, and their alloys are recognized as very promising materials for many optoelectronic device applications such as blue-green and UV light-emitting diodes (LEDs), laser diodes (LDs), UV solar blind detectors, and high-temperature/high-power electronic devices.[1] Because many III-nitride-based devices have utilized the advantages of multiple-quantum-well (MQW) structures, the optical properties of GaN/$Al_xGa_{1-x}N$ MQW structures are of great current interest.[2–10] For the optimization of LEDs and LDs structures, it is crucial to maximize the optical emission or quantum efficiencies (QEs) in the quantum-confined states in the well regions. It is expected that the QEs of MQWs depend strongly on the growth conditions. For the growth of GaN/$Al_xGa_{1-x}N$, MQWs, one can choose the growth conditions to be the optimal growth conditions of either GaN epilayers (GaN-like) or $Al_xGa_{1-x}N$ epilayers ($Al_xGa_{1-x}N$-like). It was demonstrated that the optimal growth conditions for GaN/AlGaN MQWs by metalorganic chemical-vapor deposition (MOCVD) are GaN-like.[9] On the other hand, MQW structural parameters such as well and barrier widths are expected to affect the QE as well. It was shown recently that for a fixed barrier width of 50 Å GaN/$Al_xGa_{1-x}N$ MQWs with well widths between 12 and 42 Å exhibited the highest QE.[10]

In order to bring the work along this line to a completion, we have grown a set of 30 Å well GaN/$Al_xGa_{1-x}N$ MQW structures with varying barrier widths from 30 to 100 Å. Picosecond time-resolved photoluminescence (PL) measurements have been employed to investigate the PL properties including quantum efficiency and carrier dynamics of this set of GaN/$Al_xGa_{1-x}N$ MQW structures. Our results revealed that the QE and the recombination lifetime of these 30 Å well GaN/$Al_xGa_{1-x}N$ MQWs increase with an increase of the barrier width up to 80 Å. These behaviors can be explained by two different effects in MQWs: (1) enhanced nonradiative recombination rates in MQWs of narrower barrier widths due to enhanced probabilities of the electron and hole wave functions at the interfaces as well as in the barriers (at $L_B \lesssim 80$ Å) and (2) enhanced nonradiative recombination rates in MQWs due to an increased misfit dislocation density at the interfaces when the barrier width approaches the critical thickness, $L_B \sim 100$ Å.

The GaN/$Al_xGa_{1-x}N$ $(x\approx 0.2)$ MQW samples were grown on 0001-oriented sapphire substrates under the optimal GaN-like growth conditions by MOCVD.[9,10] The MQW structure has 30 periods of GaN wells and $Al_xGa_{1-x}N$ barriers. The MQW samples were terminated by 250-Å-thick $Al_xGa_{1-x}N$ cap layers with the same composition as the barriers. The Al molar fraction in the $Al_xGa_{1-x}N$ barriers was targeted at 20%. The barrier width was targeted to vary from 30 to 100 Å. The well and barrier widths were determined by the growth rate of the GaN and $Al_xGa_{1-x}N$ epilayers under the optimal GaN-like growth conditions. The low-temperature PL spectrum for one of our representative GaN epilayers grown under the same conditions as those of the GaN wells in the MQWs studied here is shown in Fig. 1. One can see that our as-grown GaN epilayers on sapphire substrates emit only the exciton transitions at 3.483 eV with a full width at half maximum (FWHM) of about 4 meV (the ratio of the exciton emission intensity to the yellow line intensity exceeds 10^4). Picosecond time-resolved photoluminescence spectroscopy[11] was employed to study the optical properties of these MQWs. The excitation wavelength and average pumping power were 290 nm and 20 mW, respectively.

The low-temperature $(T=10\,\mathrm{K})$ PL spectra of the GaN/$Al_xGa_{1-x}N$ MQW samples with various barrier widths

[a]On leave from the Korea Research Institute of Standards and Science, Taejon 305-600, Korea.
[b]Electronic mail: jiang@phys.ksu.edu

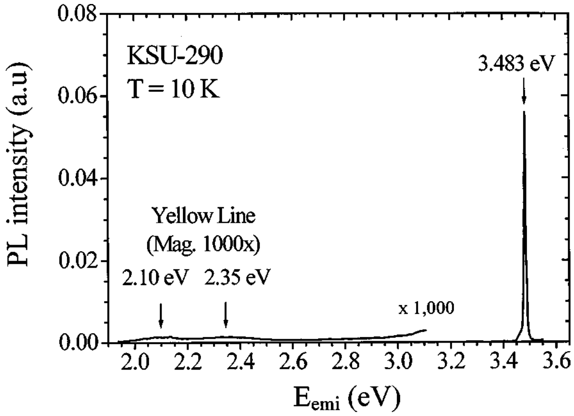

FIG. 1. Low-temperature PL spectrum for one of our undoped GaN epilayers (1.3 μm) recorded in a large emission energy scale to include yellow emission lines. The PL signal in the low-energy region ($E<3.1$ eV) has been magnified by a factor of 1000, indicating very little contribution from yellow emission and, hence, the high crystalline quality and purity of our samples.

of $L_B=30$, 40, 50, 80, and 100 Å are presented in Fig. 2. The position of the dominant emission peak at $\sim$3.56 eV (10 K) in these spectra is almost independent of the barrier width and is due to the excitonic transition from the GaN wells. The FWHM of the transition line from the wells is around $20-30$ meV, which is among the better values reported for the GaN/AlGaN MQW system.[2–10] The PL spectra also show a transition line with a lower emission intensity around 3.49 eV, which results from the underneath GaN epilayer.

One of the features exhibited by these 30 Å well MQW structures is that the excitonic transition peak resulting from the well regions is significantly blueshifted with respect to

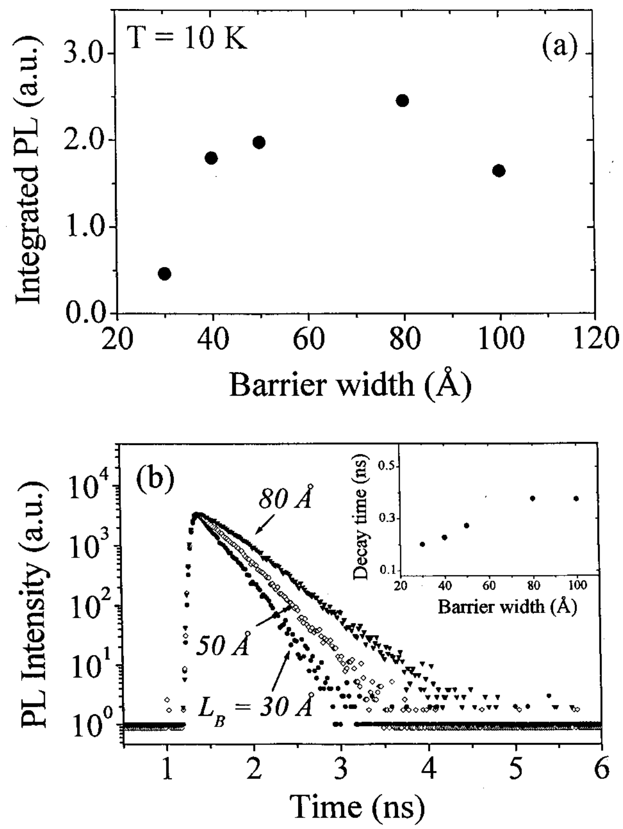

FIG. 3. (a) Integrated PL intensity of the well transition for the $GaN/Al_xGa_{1-x}N$ MQW samples as a function of L_B measured at 10 K. (b) The temporal responses of the well transitions in the $GaN/Al_xGa_{1-x}N$ MQW samples for various barrier widths at 10 K. The inset shows the barrier-width dependence of the decay lifetime for the well transition.

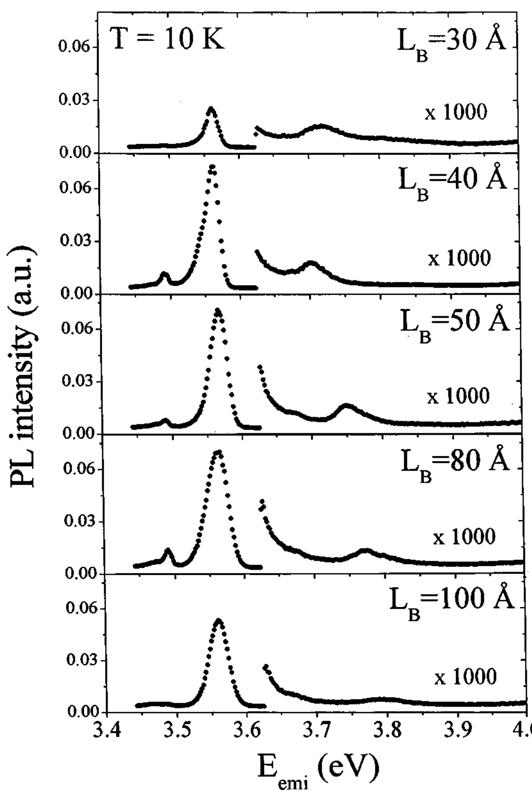

FIG. 2. cw PL spectra of a set of 30 Å well $GaN/Al_xGa_{1-x}N$ MQW samples with varying barrier widths, $L_B=30$, 40, 50, 80, and 100 Å, measured at 10 K. The MQW structures are grown under identical conditions.

the GaN epilayers by about 70 meV (10 K). The observed spectral blueshift here suggests that the quantum confinement dominates the well-known piezoelectric and polarization effects in these MOCVD-grown MQW structures. The time-resolved PL spectral peak positions of the well transitions in these samples shift toward lower emission energies by less than 10 meV as the delay time increases from 0 to 0.8 ns (not shown). The magnitude of the redshift decreases with a decrease of L_B.

Another important feature shown by these 30 Å well MQW structures is that they exhibit a ratio of well emission intensity to barrier emission intensity of about 10^4 at 10 K. Moreover, the barrier emission intensity further decreases as the temperature increases and drops to a signal level which is below the sensitivities of our detection systems when the temperature is above 200 K. This is highly preferred for laser and LED applications, since one important issue in the laser and LED structural design is to maximize the optical emission or quantum efficiency in the quantum-confined states in the well regions, while any optical transitions from the barrier regions represent a loss to optical gain.

The barrier-width dependence of the integrated PL intensity of the well transition for these 30 Å well MQW structures can also be obtained from Fig. 2, which is plotted in Fig. 3(a). The total integrated PL intensities of these MQW samples are reduced only by one order of magnitude as the temperature rises from 10 to 300 K (not shown), indicating high PL efficiencies even at room temperature. The most important result shown in Fig. 3 is that the integrated PL

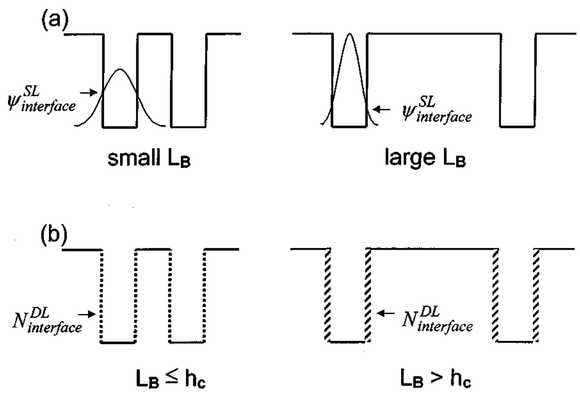

FIG. 4. (a) Schematic diagrams showing the electron wave-function distributions in MQWs for two representative barrier widths. The probability of the electron wave function at the interfaces $|\psi^{SL}|^2_{\mathrm{interface}}$ as well as in the barriers decreases with an increase of the barrier width; (b) schematic diagram showing the misfit dislocation density at the interfaces in the $GaN/Al_xGa_{1-x}N$ MQWs. The widths of the dotted lines represent the density of the misfit dislocations which increases sharply as L_B approaches h_c, where L_B and h_c denote the barrier width and the critical thickness, respectively.

intensities (or QEs) of these MQW samples increase monotonously with an increase of the barrier width up to 80 Å.

The decay lifetime for the well transitions increases almost linearly from 0.2 to 0.4 ns when the barrier width varies from 30 to 80 Å. This is clearly illustrated in Fig. 3(b), where the PL temporal responses as well as the barrier-width dependence of the PL decay lifetime are shown for the well transitions. Furthermore, a linear increase of the well transition lifetime with temperature has been observed in these MQW structures when the barrier widths are below 100 Å (not shown), which reflects that the radiative exciton recombination dominates in these MQW samples. The enhanced decay lifetime with the barrier width up to 80 Å shown in Fig. 3(b) is consistent with the QE enhancement with the barrier width shown in Fig. 3(a). For the 100 Å barrier MQW sample studied here, the well transition lifetime decreases with temperature, which is an indication of increased nonradiative recombination rates at higher temperatures in this MQW sample.

Our experimental results of the barrier-width dependence of the PL efficiency and decay lifetime can be understood in terms of the barrier-width-dependent nonradiative interface recombination rate in MQWs, R_{nr}, which can be described by

$$R_{\mathrm{nr}} \propto |\psi^{SL}|^2_{\mathrm{interface}} N^{DL}_{\mathrm{interface}}, \tag{1}$$

where $\psi^{SL}_{\mathrm{interface}}$ and $N^{DL}_{\mathrm{interface}}$ denote the electron (and hole) wave functions and the density of misfit dislocations at the interface, respectively. Thus, two distinct mechanisms predominantly control the recombination rates and, hence, the quantum efficiencies in MQW. For $L_B \lesssim 80$ Å, $N^{DL}_{\mathrm{interface}}$ does not show a strong barrier dependence. Thus, for the MQW samples with $L_B \lesssim 80$ Å, the reductions of the QE and decay lifetime with a decreased barrier width are mainly caused by an increased nonradiative recombination rate due to the enhanced probabilities of the electron and hole wave functions at the interfaces as well as in the AlGaN barriers. This situation is schematically illustrated in Fig. 4(a), where the electron wave-function distributions for two representative L_B are shown, which indicates that $\psi^{SL}_{\mathrm{interface}}$ decreases with an increase of L_B. Previously, reductions in the well emission intensities in MQWs of narrower barrier widths have been observed for the GaAs/AlGaAs MQW system.[12]

On the other hand, the decrease of the QE and the lifetime behavior in the 100 Å barrier MQW can be accounted for by the concept of critical thickness. The critical thickness h_c of the $Al_xGa_{1-x}N$ epilayers on GaN as a function of Al molar fraction x has been calculated to be around 100 Å for $x \sim 0.2$.[13–15] When L_B is approaching the critical thickness value h_c, strain is relieved by the creation of misfit dislocations at the interfaces, the situation is schematically illustrated in Fig. 4(b).

In summary, a set of $GaN/Al_xGa_{1-x}N$ MQW structures with varying barrier widths from 30 to 100 Å grown by MOCVD has been fabricated and studied by time-resolved PL measurements. The QE and recombination lifetime of these MQWs were observed to increase with the barrier width up to 80 Å. These behaviors have been explained in terms of the combined effects of a reduced probability of the electron and hole wave functions at the interfaces with an increase of L_B and an increased density of misfit dislocations at the interfaces when L_B is approaching h_c. Highly efficient emission from the wells and a ratio of the well to the barrier emission intensity of about 10^4 have been observed in these MQW structures. When utilizing the GaN/AlGaN MQWs as active media for UV light emitters, maximizing the quantum efficiency from the well regions is one of the important issues in their structural designs. Our studies have shown that the optimal GaN/AlGaN ($x \sim 0.2$) MQWs for UV light-emitter applications are those with barrier widths ranging from 40 to 80 Å and well widths ranging from 12 to 42 Å.

This research is supported by ONR, NSF (DMR-9902431 and INT-9729582), DOE (96ER45604/A000), ARO, and BMDO.

[1] H. Morkoç, S. Strite, G. B. Gao, M. E. Lin, B. Sverdlov, and M. Burns, J. Appl. Phys. **76**, 1363 (1994).
[2] M. Smith, J. Y. Lin, H. X. Jiang, A. Salvador, A. Botchkarev, W. Kim, and H. Morkoç, Appl. Phys. Lett. **69**, 2453 (1996).
[3] M. Leroux, N. Grandjean, J. Massies, B. Gil, P. Lefebvre, and P. Bigenwald, Phys. Rev. B **60**, 1496 (1998).
[4] J. S. Im, H. Kollmer, J. Off, A. Sohmer, F. Scholz, and A. Hangleiter, Phys. Rev. B **57**, R9435 (1998).
[5] P. Lefebvre, J. Allegre, B. Gil, H. Mathieu, N. Grandjean, M. Leroux, J. Massies, and P. Bigenwald, Phys. Rev. B **59**, 15363 (1999).
[6] H. Morkoç, R. Cingolani, W. Lambrecht, B. Gil, H. X. Jiang, J. Y. Lin, D. Pavlidis, and K. Shenai, MRS Internet J. Nitride Semicond. Res. **4S1**, G1.2 (1999).
[7] M. Smith, J. Y. Lin, H. X. Jiang, A. Salvador, A. Botchkarev, W. Kim, and H. Morkoç, Appl. Phys. Lett. **69**, 2453 (1996).
[8] H. S. Kim, J. Y. Lin, H. X. Jiang, W. W. Chow, A. Botchkarev, and H. Morkoç, Appl. Phys. Lett. **73**, 3426 (1998).
[9] K. C. Zeng, J. Li, J. Y. Lin, and H. X. Jiang, Appl. Phys. Lett. **76**, 864 (2000).
[10] K. C. Zeng, J. Li, J. Y. Lin, and H. X. Jiang, Appl. Phys. Lett. **76**, 3040 (2000).
[11] http://www.phys.ksu.edu/area/GaNgroup/
[12] M. Krahl, D. Bimberg, R. K. Bauer, D. E. Mars, and J. N. Miller, J. Appl. Phys. **67**, 434 (1990).
[13] J. Qu, J. Li, and G. Zhang, Solid State Commun. **107**, 467 (1998).
[14] W. G. Perry, M. B. Bremser, T. Zheleva, K. J. Linthicum, and R. F. Davis, Thin Solid Films **324**, 107 (1998).
[15] S. Krishnankutty, R. M. Kolbas, M. Asif Khan, J. N. Kuznia, J. M. Van Hove, and D. T. Olson, J. Electron. Mater. **21**, 437 (1992).